Resonant two-photon ionization spectroscopy of BNB

Hongbin Ding, Michael D. Morse,[a] Cristina Apetrei, Lukasz Chacaga, and John P. Maier
Departement Chemie, Universität Basel, Klingelbergstrasse 80, CH-4056 Basel, Switzerland

(Received 5 September 2006; accepted 16 October 2006; published online 20 November 2006)

Triatomic BNB has been produced by laser ablation of a boron nitride rod in a supersonic expansion of helium carrier gas and has been investigated using resonant two-photon ionization spectroscopy in the visible region. The $\tilde{B}\,^2\Pi_g - \tilde{X}\,^2\Sigma_u^+$ band system has been recorded near 514 nm and is dominated by a strong origin band, which has been rotationally resolved and analyzed. Both the $^{11}B^{14}N^{11}B$ (64% natural abundance) and the $^{10}B^{14}N^{11}B$ (32% natural abundance) isotopic modifications have been analyzed, leading to the spectroscopic constants (and their 1σ error limits) of $B_0''(\tilde{X}\,^2\Sigma_u^+)=0.466\,147(70)$, $B_0'(\tilde{B}\,^2\Pi_g)=0.467\,255(75)$, and $A_0'(\tilde{B}\,^2\Pi_g)=6.1563(38)$ cm^{-1} for $^{10}B^{14}N^{11}B$, corresponding to $r''_{B-N}(\tilde{X}\,^2\Sigma_u^+)=1.312\,47(10)$ Å and $r'_{B-N}(\tilde{B}\,^2\Pi_g)=1.310\,92(11)$ Å. Very similar values are obtained for the more abundant isotopomer, $^{11}B^{14}N^{11}B$: $B_0''(\tilde{X}\,^2\Sigma_u^+)=0.444\,493(69)$, $B_0'(\tilde{B}\,^2\Pi_g)=0.445\,606(70)$, $A_0'(\tilde{B}\,^2\Pi_g)=6.1455(38)$ cm^{-1}, corresponding to $r''_{B-N}(\tilde{X}\,^2\Sigma_u^+)=1.312\,41(10)$ Å and $r'_{B-N}(\tilde{B}\,^2\Pi_g)=1.310\,77(10)$ Å. These results are discussed as they relate to Walsh's rules and are compared to results for related molecules. © *2006 American Institute of Physics*. [DOI: 10.1063/1.2390713]

I. INTRODUCTION

In 1953, Walsh investigated the molecular orbitals of triatomic *p*-block molecules and their correlation as the molecular geometry is distorted from linear to bent.[1] This work led to Walsh's rules, which are widely used to predict the equilibrium ground state geometry of triatomic molecules.[2,3] For a triatomic nonhydride, AB_2, Walsh predicted that the molecule will be linear if it contains 16 or fewer valence $(ns+np)$ electrons and bent if it contains 17–20 valence electrons, becoming more strongly bent as the number of valence electrons increases.[1] When the number of valence electrons is increased to 22, the molecule becomes linear again. In this scheme BNB has 11 valence electrons and is predicted to be linear in its ground state.

Walsh's rules have been tested on a large number of stable molecules, radicals, and ions, and have been found to be generally accurate in predicting the geometries of molecules with 12 or more valence electrons. Among the $2s$, $2p$ series of neutral triatomic molecules, experimental structural determinations have been made for Li_3 (with three valence electrons);[4] Li_2O (8 e^-);[5] B_3 (9 e^-);[6] LiNC (10 e^-);[7] C_3 (12 e^-);[8] CCN and CNC (13 e^-);[9,10] CCO, NCN, and CNN (14 e^-);[11–13] BO_2, NCO, and N_3 (15 e^-);[14–16] FCN, CO_2, and N_2O (16 e^-);[17–19] FCO and NO_2 (17 e^-);[20,21] CF_2, FNO, and O_3 (18 e^-);[22–24] NF_2 and FO_2 (19 e^-);[25,26] and OF_2 (20 e^-).[27] Of these, all of the species with 17 or more valence electrons are bent, and all of the species with 10–16 valence electrons are linear in their ground electronic states, exactly in accord with Walsh's rule. The triatomic Li_3 (three electrons),[4] however, has a Jahn-Teller distorted equilateral triangular structure, while B_3 (9 e^-) has an undistorted equilateral structure, thereby violating Walsh's rule.[6] The eight electron molecule, Li_2O, is linear.[5] To date, no 11-electron molecules have been structurally investigated in detail and our study of BNB is designed, in part, to fill this gap.

Triatomic BNB has been previously investigated using a variety of spectroscopic and calculational methods, and it is generally agreed that it is linear in its ground electronic state. A matrix isolation electron spin resonance (ESR) investigation, conducted in solid neon, argon, and krypton matrices in 1992, demonstrated convincingly that the ground state in these matrices is an $\tilde{X}\,^2\Sigma$ state.[28] Hyperfine splittings due to both the ^{11}B and ^{14}N nuclei (and in the case of the $^{10}B^{14}N^{11}B$ molecule, due to the ^{10}B nucleus as well) were observed and measured. The results were analyzed according to the free atom comparison method,[29] and the unpaired electron was found to have 18% $2s$ and 27% $2p$ character on each boron atom and −1% $2s$ and 11% $2p$ character on the nitrogen atom. The −1% $2s$ character on the nitrogen atom is obviously an artifact of the method, but the small, nearly zero value obtained in the analysis suggests negligible $2s_N$ participation in the singly occupied σ orbital. The negligible $2s_N$ character and significant $2p\sigma_N$ character imply that the unpaired electron is in an orbital of σ_u symmetry, and provides convincing evidence that the ground state is an $\tilde{X}\,^2\Sigma_u^+$ term.

Infrared absorption bands have been observed in matrix isolation studies of laser-ablated boron nitride or of laser-ablated elemental boron reacting with N_2 or NH_3, and some of these have been attributed to the cyclic (C_{2v}) and linear isomers of BNB.[30–32] Identifications were based on the isotope shifts, annealing behavior, and comparisons to *ab initio* calculations. Strong infrared absorptions were also observed in the cryogenic argon matrix near 6000 cm^{-1}, due to the $\tilde{A}\,^2\Sigma_g^+ - \tilde{X}\,^2\Sigma_u^+$ electronic band system.[31] The $\tilde{A}\,^2\Sigma_g^+$ state was

[a]Also at Department of Chemistry, University of Utah, Salt Lake City, UT 84112. Electronic mail: morse@chem.utah.edu

also observed in photoelectron spectroscopic (PES) studies of mass-selected B_2N^- anions, placing the zero-point level of the $\tilde{A}\,^2\Sigma_g^+$ state 6330 ± 40 cm^{-1} above the ground level of the $\tilde{X}\,^2\Sigma_u^+$ state.[33] In the photoelectron investigation, vibrational intervals in the $\tilde{X}\,^2\Sigma_u^+$ ground state were observed that matched those found in the matrix isolation study, but it was not necessary to invoke the existence of a cyclic form of the molecule. The σ_u antisymmetric stretching mode, ν_3, is found to have an anomalously low fundamental frequency (855 ± 40 cm^{-1}) due to Herzberg-Teller coupling of the ground $\tilde{X}\,^2\Sigma_u^+$ state with the low-lying $\tilde{A}\,^2\Sigma_g^+$ state. Herzberg-Teller vibronic coupling also transfers intensity from the electronically allowed $\tilde{A}\,^2\Sigma_g^+-\tilde{X}\,^2\Sigma_u^+$ band system to the overtones of the σ_u antisymmetric stretching vibration (ν_3), causing the $(0\ 0^0\ 3)$ and $(0\ 0^0\ 5)$ levels to gain intensity in transitions from the $(0\ 0^0\ 0)$ ground vibronic state, as observed in the matrix isolation spectra.[31] Based on the reassignment reported in the PES investigation, it appears that there is no evidence of a low-lying cyclic form of BNB in either the matrix or gas phase work. Knudsen effusion mass spectrometry has been used to establish that the atomization energy of BNB is 10.8 ± 0.2 eV, making BNB quite a strongly bound molecule.[34]

Triatomic BNB also presents a challenge to computational chemistry that is surprising given that the molecule has only 17 electrons.[35–41] While all of the computational methods show that the ground state of BNB is the linear $\tilde{X}\,^2\Sigma_u^+$ state, vibronic interaction with the $\tilde{A}\,^2\Sigma_g^+$ state introduces problems in estimating the frequency of the antisymmetric stretching motion. In some calculations, the molecule breaks symmetry to form a $C_{\infty v}$ structure with one long bond and one short bond,[33,37,39] and the issue of whether this symmetry breaking is real or artifactual has been a subject of debate.[39,41] In addition, the ground state of BNB exhibits a very low-frequency bending motion, with calculated bending frequencies lying in the range of 73–153 cm^{-1}.[41] Cuts through the multidimensional potential energy surface along the bending coordinate[38] and along the antisymmetric stretching coordinate[33,41] show curves that look more like a square well than a harmonic potential.

Despite all of this interest in BNB, no published gas phase spectra have been reported, other than the photoelectron study. Here we provide a study of the $\tilde{B}\,^2\Pi_g-\tilde{X}\,^2\Sigma_u^+$ band system, in which we have rotationally resolved and analyzed the origin band, thereby determining the vibrationally averaged B–N bond length of both the $\tilde{X}\,^2\Sigma_u^+$ and the $\tilde{B}\,^2\Pi_g$ electronic states along with other spectroscopic parameters.

II. EXPERIMENT

The experiment was performed using the resonance enhanced two-color two-photon ionization (R2C2PI) spectrometer in Basel, which has been previously described.[42] A molecular beam was produced by laser ablation of a boron nitride rod in the throat of a pulsed supersonic expansion of helium or neon carrier gas at a backing pressure of ~5 bars using 30 mJ/pulse of the 532 nm radiation from a pulsed Nd:YAG laser for ablation. The products of ablation were entrained in the carrier gas and cooled in the ensuing supersonic expansion. The expansion was skimmed to form a well-collimated beam of neutral and ionized molecules. Ions were removed from the beam by a perpendicular electric field before entering the ionization region of a Wiley-McLaren time-of-flight mass spectrometer,[43] where the molecules were irradiated with a pulse of tunable visible radiation produced by either an optical parametric oscillator-optical parametric amplifier (OPO-OPA) laser system or an excimer-pumped dye laser. Following a short delay the molecules were exposed to a pulse of 157 nm radiation produced by an excimer laser operating on the F_2 transition. To prevent atmospheric absorption, the beam path of the F_2 laser radiation was flushed with N_2. The combination of the visible and the deep UV photons was sufficient to ionize the BNB molecule. Ion signal was collected at the masses of $^{10}B^{14}N^{10}B$ (mass 34), $^{10}B^{14}N^{11}B$ (mass 35), and $^{11}B^{14}N^{11}B$ (mass 36) as the visible laser was scanned, thereby providing spectra of the BNB isotopomers. In addition to BNB, large clusters were also produced, evidenced by the observation of signal at every mass between 100 and 200 Da.

Low resolution survey scans were conducted using the OPO-OPA laser system; for the rotationally resolved work, a pulsed dye laser was used with an intracavity étalon to narrow the laser linewidth to approximately 0.05 cm^{-1}. The resulting spectra were calibrated by collecting the laser-induced fluorescence spectrum of I_2 vapor simultaneously with the BNB spectrum, and using the I_2 atlas to identify the lines.[44,45] Standard deviations in the fits of the measured I_2 lines were below 0.01 cm^{-1}, with maximum absolute errors below 0.025 cm^{-1}. The accuracy of the measured BNB line positions is therefore thought to be better than 0.025 cm^{-1}. Because the dye laser was counterpropagated down the molecular beam axis, the BNB molecules were moving toward the light source at the beam velocity, which for helium carrier gas is about 1.77×10^5 cm s^{-1}. This leads to a Doppler shift, causing the BNB molecules to experience the excitation radiation blueshifted by approximately 0.115 cm^{-1}. This correction has been applied to all of the measured lines of BNB.

III. RESULTS

A. Vibronic spectrum of BNB

The spectrum of BNB was investigated over the range of 400–700 nm, but vibronic bands were found only in the 470–510 nm range. Figure 1 displays the spectrum obtained by laser ablation of a BN rod into helium carrier gas. The spectrum could also be observed using neon carrier gas, but the overall intensity was reduced and many of the bands could not be observed. Table I provides a list of the vibronic bands observed, along with isotope shift information.

The band system is dominated by the origin band, indicating that there is little change in equilibrium bond lengths or angles upon electronic excitation. This conclusion is borne out in the analysis of the rotationally resolved spectrum, which is presented in Sec. III B below. The results of the rotational analysis show that the separation between the B

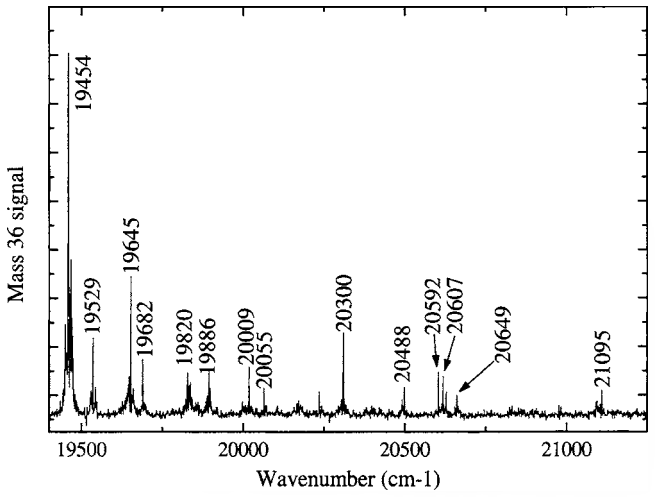

FIG. 1. Vibronically resolved scan of the $\tilde{B}\,^2\Pi_g - \tilde{X}\,^2\Sigma_u^+$ band system of $^{11}B^{14}N^{11}B$. Wave numbers of the major features are given.

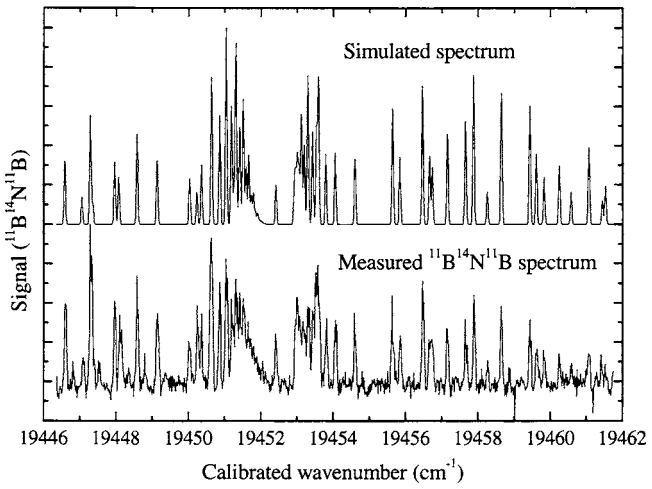

FIG. 2. Rotationally resolved scan over the central portion of the origin band of the $\tilde{B}\,^2\Pi_g - \tilde{X}\,^2\Sigma_u^+$ band system of $^{11}B^{14}N^{11}B$ (lower panel) and the simulated spectrum (upper panel). Nuclear spin statistics for identical $I=3/2$ ^{11}B nuclei are included in the simulated spectrum.

and N atoms in the BNB structure changes from 1.3124(1) Å in the $\tilde{X}\,^2\Sigma_u^+$ ground state to 1.3108(1) Å in the $\tilde{B}\,^2\Pi_g$ excited state.

The vibronically resolved spectrum that is displayed in Fig. 1 is not readily assigned. In part, this is due to some hot bands that are observed when helium carrier gas is used. In addition, the $\tilde{B}\,^2\Pi_g$ excited state is subject to the Renner-Teller effect, leading to a complicated pattern of bending vibrational levels that we have not yet sorted out. Analysis of the vibronic structure of the $\tilde{B}\,^2\Pi_g - \tilde{X}\,^2\Sigma_u^+$ band system will be the focus of another article.

B. Rotationally resolved investigations

Figure 2 presents a portion of the origin band of $^{11}B^{14}N^{11}B$ that was rotationally resolved with the aid of the intracavity étalon, along with a simulation of the spectrum

TABLE I. Vibronic bands of the $\tilde{B}\,^2\Pi_g - \tilde{X}\,^2\Sigma_u^+$ system of BNB.

Wave number of band (cm^{-1})		Isotope shift (cm^{-1})	Comment
$^{11}B^{14}N^{11}B$	$^{10}B^{14}N^{11}B$		
19 454	19 457	3	Origin band, displayed in Fig. 2
19 529	19 532	3	
19 645	19 650	5	
19 682	19 688	6	
19 820	19 827	7	
19 886	19 893	7	
20 009	20 018	9	
20 055	20 064	9	
20 162	20 172	10	
20 226			
20 300	20 312	12	
20 488			
20 592			
20 607			
20 649			
21 095	21 116	21	

based on the least-squares fit of the lines. To obtain a fit of the spectrum, it was accepted that the ground state of BNB is the $\tilde{X}\,^2\Sigma_u^+$ state, as found in all *ab initio* studies[35–41] and in the ESR investigation.[28] Given that the ground state is of $^2\Sigma_u^+$ symmetry, the only candidates for the excited state would be of either $^2\Sigma_g^+$ or $^2\Pi_g$ symmetry. The spectrum is clearly too complicated for a $^2\Sigma_g^+ - \tilde{X}\,^2\Sigma_u^+$ system, so a $^2\Pi_g - ^2\Sigma_u^+$ system was considered.

Using a B'' value obtained from the *ab initio* bond lengths and a spin-rotation constant, γ'', obtained by applying the Curl relationship[46] to the g tensor reported in the ESR study,[28] reasonable starting parameters for a spectral simulation were obtained for the ground state. The nearly symmetric pattern of the two inner branches (lying between 19 450 and 19 454 cm^{-1}) suggested that the upper and lower state B values are similar, thereby allowing B' to be estimated as well. To estimate the likely magnitude of the spin-orbit constant, $A'(\tilde{B}\,^2\Pi_g)$, we recognized that a π_g orbital in this molecule can have no $2p$ contribution on the central nitrogen atom because a $2p_\pi$ orbital on this atom will be of *ungerade* symmetry. Therefore, the singly occupied π_g orbital is likely well approximated as $|\pi_g\rangle = 1/\sqrt{2}[|2p_{\pi B1}\rangle - |2p_{\pi B2}\rangle]$. Using atomic $2p$ orbitals for boron and the spin-orbit operator, it is straightforward to estimate the spin-orbit constant for the $\tilde{B}\,^2\Pi_g$ state as $A'(\tilde{B}\,^2\Pi_g) \approx \zeta_{2p}(B) = 10.7$ cm^{-1}.[47] A simulation of the spectrum using these initial guesses gave a separation between the two inner branches that was clearly too large, so A' was reduced. As the value of A' was reduced, eventually the line assignment became obvious so that a least-squares fit of the spectroscopic constants to the measured line positions could be made. Simulation and fitting of the spectrum were performed using PGOPHER, a program written by Colin Western that is freely available on the internet.[48] The measured line positions and the residuals in the fit are provided in Table II for both the $^{10}B^{14}N^{11}B$ (mass 35) and $^{11}B^{14}N^{11}B$ (mass 36) isotopomers. The derived spectroscopic constants are given in Table III.

TABLE II. Measured and fitted line positions for the $\tilde{B}\,^2\Pi_g - \tilde{X}\,^2\Sigma_u^-$ 0-0 band of BNB. Residuals in the least-squares fit are given in parentheses for each line, in units of 0.0001 cm^{-1}.

Line	$^{10}B^{14}N^{11}B$	$^{11}B^{14}N^{11}B$	Line	$^{10}B^{14}N^{11}B$	$^{11}B^{14}N^{11}B$
$P_1(5/2)$	19 451.8636(−42)	19 448.7013(12)	$Q_{21}(7/2)$	19 460.5824(−64)	
$P_1(7/2)$	19 451.2179(36)	19 448.0810(−42)	$Q_{12}(1/2)$	19 452.4334(−217)	19 449.2621(77)
$P_1(9/2)$	19 450.5021(−37)	19 447.4223(32)	$Q_{12}(3/2)$	19 451.8636(−69)	19 448.7013(−15)
$P_1(11/2)$	19 449.7643(94)	19 446.7080(−46)	$Q_{12}(5/2)$	19 451.2179(−2)	19 448.0810(−81)
$P_1(13/2)$	19 448.9928(208)	19 445.9683(−68)	$Q_{12}(7/2)$	19 450.5021(−87)	19 447.4223(−18)
$P_1(15/2)$	19 448.1651(−2)	19 445.2383(241)	$Q_{12}(9/2)$	19 449.7643(33)	19 446.7080(−106)
$P_1(17/2)$	19 447.3436(25)	19 444.4453(95)	$Q_{12}(11/2)$	19 448.9936(144)	19 445.9683(−140)
$P_1(19/2)$	19 446.4941(−98)	19 443.6213(−231)	$Q_{12}(13/2)$		19 445.2383(158)
$P_1(21/2)$	19 445.6539(−34)	19 442.8453(22)	$Q_2(3/2)$	19 457.3250(−119)	19 454.1703(−87)
$P_1(23/2)$	19 444.8017(−19)	19 442.0233(−113)	$Q_2(5/2)$	19 457.0520(−173)	19 453.9203(44)
$P_1(25/2)$	19 443.9400(−49)	19 441.2303(95)	$Q_2(7/2)$	19 456.8734(124)	
$P_1(27/2)$	19 443.0855(29)	19 440.3863(−169)	$Q_2(11/2)$	19 456.5822(75)	19 453.4043(−145)
$P_1(29/2)$		19 439.5923(94)	$R_1(3/2)$	19 455.8799(30)	19 452.5273(−39)
$P_1(31/2)$	19 441.3675(160)	19 438.7743(135)	$R_1(5/2)$	19 457.0520(190)	19 453.6368(−63)
$P_1(33/2)$	19 440.4784(−58)	19 437.9343(33)	$R_1(7/2)$	19 458.1531(64)	19 454.7158(12)
$P_1(35/2)$	19 439.6080(−86)		$R_1(9/2)$	19 459.2087(−196)	19 455.7493(−58)
$P_{12}(3/2)$	19 450.5769(−141)		$R_1(11/2)$	19 460.2877(14)	19 456.7780(58)
$P_{12}(5/2)$	19 449.0512(−225)		$R_1(13/2)$	19 461.3480(214)	19 457.7683(−34)
$P_{12}(7/2)$	19 447.5052(173)		$R_1(15/2)$	19 462.3744(204)	19 458.7566(−16)
$P_{12}(9/2)$	19 445.8483(19)	19 442.9713(−68)	$R_1(17/2)$	19 463.3637(−82)	19 459.7446(97)
$P_{12}(11/2)$	19 444.1562(−55)	19 441.4103(286)	$R_1(19/2)$	19 464.3895(66)	19 460.6953(−91)
$P_{12}(13/2)$	19 442.4313(−128)	19 439.7783(246)	$R_1(21/2)$	19 465.3771(−117)	19 461.6903(217)
$P_{12}(15/2)$	19 440.6987(−33)	19 438.1033(17)	$R_1(23/2)$	19 466.3944(33)	19 462.6260(−30)
$P_{12}(17/2)$	19 438.9467(52)		$R_1(25/2)$	19 467.3758(−151)	19 463.5820(−46)
$P_{12}(19/2)$	19 437.1857(184)	19 434.7373(−98)	$R_1(27/2)$		19 464.5500(75)
$P_{12}(21/2)$	19 435.3764(−65)	19 433.0713(187)	$R_{21}(3/2)$	19 461.7283(3)	19 458.3746(165)
$P_{12}(23/2)$	19 433.5865(−43)		$R_{21}(5/2)$	19 463.3637(−195)	19 459.9396(121)
$P_2(7/2)$	19 453.3447(27)	19 450.3548(−69)	$R_{21}(7/2)$	19 465.0891(38)	19 461.5546(127)
$P_2(9/2)$	19 452.1937(−94)	19 449.2621(−46)	$R_{21}(9/2)$	19 466.8156(−82)	19 464.8806(114)
$P_2(11/2)$	19 451.1177(57)	19 448.2173(−1)	$R_{21}(11/2)$	19 468.6004(98)	19 466.5726(39)
$P_2(13/2)$	19 450.0587(6)	19 447.2090(48)	$R_{21}(13/2)$	19 470.3738(−55)	19 468.2790(−68)
$P_2(15/2)$	19 449.0512(180)	19 446.1963(−232)	$R_{21}(15/2)$	19 472.1752(−102)	19 470.0133(−39)
$P_2(17/2)$	19 448.0290(−21)	19 445.2383(−193)	$R_{21}(17/2)$	19 474.0045(−9)	19 473.5063(−66)
$P_2(19/2)$	19 447.0535(64)	19 444.3173(35)	$R_{21}(19/2)$	19 475.8366(−2)	
$P_2(21/2)$	19 446.0628(−150)	19 443.3743(−106)	$R_2(1/2)$	19 459.2087(74)	19 455.9668(100)
$P_2(23/2)$	19 445.1280(73)	19 442.4643(−40)	$R_2(3/2)$	19 459.8756(87)	19 456.5898(63)
$P_2(25/2)$	19 444.1562(−175)	19 441.5663(43)	$R_2(5/2)$	19 460.5841(−86)	19 457.2686(21)
$P_2(27/2)$	19 443.2416(61)		$R_2(7/2)$	19 461.3480(−182)	19 457.9956(5)
$Q_1(1/2)$		19 450.1401(−24)	$R_2(9/2)$	19 462.1831(62)	19 458.7566(−33)
$Q_1(3/2)$	19 453.7326(2)	19 450.4743(−45)	$R_2(11/2)$	19 463.0145(−20)	19 459.5576(44)
$Q_1(5/2)$	19 454.0018(−83)	19 450.7356(−167)	$R_2(13/2)$	19 463.8853(63)	19 460.3656(−36)
$Q_1(7/2)$	19 454.2315(−6)	19 450.9686(−54)	$R_2(15/2)$	19 464.7672(76)	19 461.1988(−46)
$Q_1(9/2)$	19 454.4284(176)	19 451.1728(183)	$R_2(17/2)$	19 465.6351(−198)	19 462.0616(92)
$Q_1(11/2)$	19 454.5687(119)	19 451.2983(−50)	$R_2(19/2)$	19 466.5784(161)	19 462.9076(−62)
$Q_1(13/2)$	19 454.6633(−148)	19 451.4108(−173)	$R_2(21/2)$	19 467.4762(−38)	19 463.7910(54)
$Q_1(15/2)$	19 454.7732(−80)	19 451.5293(−53)	$R_2(23/2)$	19 468.3953(−111)	19 464.6713(51)
$Q_1(17/2)$	19 454.8855(150)	19 451.6313(39)	$R_2(25/2)$	19 469.3639(235)	
$Q_{21}(3/2)$	19 459.2108(111)		$R_2(27/2)$		19 466.4398(−102)
$Q_{21}(5/2)$	19 459.8776(134)				

The fitted value of A' (6.15 cm^{-1}) is only 57% of the predicted value of 10.7 cm^{-1}. Such a sizable departure is surprising. If the charge distribution were such that the B atoms were negatively charged, this could reduce the A' value, since the value of $\zeta_{2p}(B^-)$ is only 5.3 cm^{-1}. An *ab initio* calculation of the $\tilde{B}\,^2\Pi_g$ state, to be reported in a subsequent publication, shows a charge of only −0.06 on the B atoms, however, making it unlikely that this is the cause of the small spin-orbit constant. Another possibility is that configuration interaction mixes the $\tilde{B}\,^2\Pi_g$ state strongly with another state that reduces the spin-orbit constant. A final possibility is that the Renner-Teller splitting of the two components of the $^2\Pi_g$ state reduces the vibrationally averaged value of the spin-orbit constant. In our opinion, this is

TABLE III. Fitted spectroscopic constants of BNB.

State	Constant	$^{10}B^{14}N^{11}B$	$^{11}B^{14}N^{11}B$
$\tilde{X}\,^2\Sigma_u^+$	B_0 (cm^{-1})	0.466 147(70)	0.444 493(69)
	γ (cm^{-1})[a]	0.0011 (held fixed)	0.0011 (held fixed)
	r_0(B–N) (Å)	1.312 47(10)	1.312 41(10)
$\tilde{B}\,^2\Pi_g$	T_0 (cm^{-1})	19 455.5299(19)	19 452.3239(19)
	B_0 (cm^{-1})	0.467 255(75)	0.445 606(70)
	A_0 (cm^{-1})	6.1563(38)	6.1455(38)
	p_0 (cm^{-1})	$-8.0(6.1)\times10^{-4}$	$-3.5(5.8)\times10^{-4}$
	q_0 (cm^{-1})	$3.52(56)\times10^{-4}$	$2.99(56)\times10^{-4}$
	r_0(B–N) (Å)	1.310 92(11)	1.310 77(10)

[a]When γ'' was allowed to vary, it was not well determined. Therefore, it was fixed at the value obtained from the Curl relationship, which is probably more accurate than any value that might be determined from this work.

the most likely explanation for the small magnitude of the A' constant in the $\tilde{B}\,^2\Pi_g$ state of BNB.

It should be mentioned that the rotational analysis procedure was not quite as straightforward as described above because additional lines appear in the rotationally resolved spectrum when the pulsed dye laser power is too high. This is in contrast to the usual situation, in which a high power simply leads to power broadening and a loss of spectral resolution. The extra lines showed every sign of belonging to the spectrum of the origin band, since they were of similar intensity to the lines that were eventually assigned and fitted. Further, they appeared in the spectra of both isotopomers, although not in the same place relative to the band origin. The extra lines arise from a second BNB absorption band that overlaps with the origin band. We have not determined whether they arise from the ground level of the $\tilde{X}\,^2\Sigma_u^+$ state or from a vibrationally excited level of this state. In either case, the transition moment for this second band, including the Franck-Condon factor, is considerably weaker than that of the origin band, so it is possible to discriminate against these extra lines by reducing the intensity of the laser radiation.

The spectrum for the $^{11}B^{14}N^{11}B$ molecule displays nuclear spin statistics, as expected for a molecule with equivalent ^{11}B ($I=3/2$) nuclei. This leads to an intensity alternation of 5:3, with levels corresponding to even values of N'' showing greater intensity than those with odd values of N''. Thus, the F_1'' components with $J''=$even integer$+1/2$ are more intense, those with $J''=$odd integer$+1/2$ are less intense. This behavior is reversed for the F_2'' components. The pattern of intensity alternation is most evident in Fig. 2 in the $Q_1(J)$ branch, between 19 450 and 19 452 cm^{-1}. The sense of the nuclear spin statistics is as expected for an $\tilde{X}\,^2\Sigma_u^+$ ground state (or for an $\tilde{X}\,^2\Sigma_g^-$ ground state). Since the latter is ruled out by the ESR data, we consider the nuclear spin statistics to be a definitive confirmation of the $\tilde{X}\,^2\Sigma_u^+$ ground state symmetry.

The spectrum for the $^{10}B^{14}N^{11}B$ isotopomer, displayed in Fig. 3, shows no intensity alternation, as expected. A comparison to the spectrum of the $^{11}B^{14}N^{11}B$ isotopomer illustrates the difference in line intensities that are induced by the presence of identical $I=3/2$ nuclei. In Figs. 2 and 3, both simulated spectra include the effects of nuclear spin statistics, as appropriate.

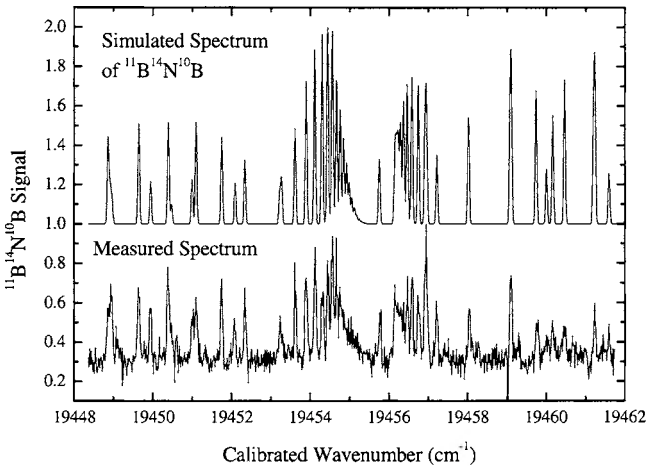

FIG. 3. Rotationally resolved scan over the central portion of the origin band of the $\tilde{B}\,^2\Pi_g-\tilde{X}\,^2\Sigma_u^+$ band system of $^{10}B^{14}N^{11}B$ (lower panel) and the simulated spectrum (upper panel). Because there are no identical nuclei in this molecule, lines are weighted equally in the simulated spectrum.

IV. DISCUSSION

A. Centrosymmetry, or the lack thereof

Triatomic BNB has been shown to have an $\tilde{X}\,^2\Sigma_u^+$ ground state, with vibrationally averaged B–N bond lengths of 1.3124 Å. Unfortunately, this work provides no data concerning whether the ground state is precisely linear or quasilinear, or whether the geometry at the potential minimum is symmetry broken to form a $C_{\infty v}$ structure, as has been predicted in some *ab initio* calculations.[33,37,39] To decide these issues, a study of the vibrational levels of the ground electronic state would be required, combined with modeling of the potential energy surface.

It can be stated with certainty that if the molecule has a barrier at the centrosymmetric structure, the barrier is not extraordinarily high. If a high barrier were present, the $(0,0^0,1)$ vibrational level of the ground $\tilde{X}\,^2\Sigma_u^+$ state would lie quite close to the $(0,0^0,0)$ level, and would be thermally populated. Transitions from this level would be strongly observed in the spectrum, and they would display the opposite intensity alternation as is observed in the origin band. No strong transitions of this type are present. If the molecule had a high barrier at the centrosymmetric configuration in both the ground $\tilde{X}\,^2\Sigma_u^+$ state and in the excited $\tilde{B}\,^2\Pi_g$ state, then the $(0,0^0,0)\leftarrow(0,0^0,0)$ and $(0,0^0,1)\leftarrow(0,0^0,1)$ transitions would overlap, and for a sufficiently high barrier, the rotational lines of the two bands would precisely overlap, resulting in an apparent cancellation of the intensity alternation. In such a situation, it would appear that the two ^{11}B nuclei are in distinguishable environments. Based on the observed spectra, this is not the case either.

To decide whether a barrier exists at the centrosymmetric configuration, the energies of the $(0,0^0,\nu_3)$ levels in the ground $\tilde{X}\,^2\Sigma_u^+$ state would have to be measured, and the re-

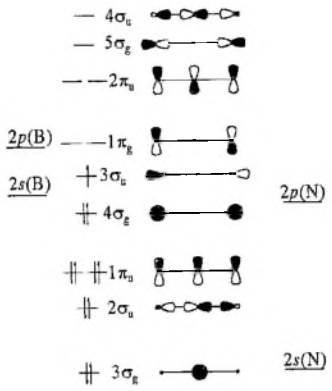

FIG. 4. Qualitative molecular orbital diagram for BNB and related molecules.

sulting set of levels used to deduce the potential function along the antisymmetric stretching coordinate, Q_3. For even values of ν_3, this would be possible in principle by either dispersed fluorescence or stimulated emission pumping spectroscopy. In practice, however, it appears that these levels will be difficult to reach owing to poor Franck-Condon factors. For odd values of ν_3, a direct infrared absorption study provides the best method for the accurate measurement of the levels. Measurements of the $(0,0^0,1)$, $(0,0^0,2)$, $(0,0^0,3)$, $(0,0^0,5)$ levels have been reported using photoelectron spectroscopy, with error limits of $\pm 40\ \mathrm{cm}^{-1}$.[33] Analysis of these vibrational levels supports the idea that a small barrier (approximately $18\ \mathrm{cm}^{-1}$) may exist at the centrosymmetric configuration.[33] To clarify this situation, more accurate measurements of the $(0,0^0,\nu_3)$ levels in the interacting $\tilde{X}\,^2\Sigma_u^+$ and $\tilde{A}\,^2\Sigma_g^+$ states would be very desirable.

B. Electronic structure and Walsh's rule

As far as we are aware, BNB is the first of the 11 valence electron *p*-block triatomics to have been investigated with rotational resolution in the gas phase. Its electronic structure can be understood, in simple terms, by considering the molecular orbital diagram displayed in Fig. 4. In this diagram, the orbitals based on the B and N 1*s* (core) orbitals are not shown, although they are included in the numbering scheme. The $2s_N$ orbital is considered to be primarily corelike and forms the $3\sigma_g$ orbital, although, of course, some mixing of the $2s_N$ orbital into the other σ_g orbitals is expected. The $2\sigma_u$ orbital is a bonding combination of the $2p\sigma$ orbital on the central nitrogen atom with $2sp\sigma$ hybrid orbitals on the two borons. The $1\pi_u$ orbital is a bonding combination of all $2p\pi$ orbitals on all three atoms, while the $4\sigma_g$ and $3\sigma_u$ orbitals are close lying and not strongly bonding in character. The small separation of these two orbitals accounts for the small energy required to promote the molecule from the $3\sigma_g^2 2\sigma_u^2 1\pi_u^4 4\sigma_g^2 3\sigma_u^1$, $\tilde{X}\,^2\Sigma_u^+$ ground state to the $3\sigma_g^2 2\sigma_u^2 1\pi_u^4 4\sigma_g^1 3\sigma_u^2$, $\tilde{A}\,^2\Sigma_g^+$ state at $6330\ \mathrm{cm}^{-1}$.[33] A larger gap exists between the $3\sigma_u$ and $1\pi_g$ orbitals, thereby placing the transition to the $3\sigma_g^2 2\sigma_u^2 1\pi_u^4 4\sigma_g^2 1\pi_g^1$, $\tilde{B}\,^2\Pi_g$ state much higher in energy, at $19\,452\ \mathrm{cm}^{-1}$. Nevertheless, the nonbonding character of the $1\pi_g$ and $3\sigma_u$ orbitals implies no significant change in B–N bond lengths in this transition, as is observed.

Adding an additional electron to form a 12-electron molecule, such as C_3, the ground electronic configuration becomes $3\sigma_g^2 2\sigma_u^2 1\pi_u^4 4\sigma_g^2 3\sigma_u^2$, $\tilde{X}\,^1\Sigma_g^+$, as is well known.[49] The 13-electron molecules CCN and CNC then begin to fill the $1\pi_g$ orbital, leading to ground configurations of $3\sigma_g^2 2\sigma_u^2 1\pi_u^4 4\sigma_g^2 3\sigma_u^2 1\pi_g^1$, $\tilde{X}\,^2\Pi_g$. Of course, the g/u designation must be dropped for molecules that lack a center of inversion. Since the $1\pi_g$ orbital only contains one electron, both CCN and CNC are expected to have a regular spin-orbit structure, as observed.[9,10] The 14-electron molecules CCO, NCN, and CNN all continue filling the $1\pi_g$ orbital, leading to a high spin ground state: $3\sigma_g^2 2\sigma_u^2 1\pi_u^4 4\sigma_g^2 3\sigma_u^2 1\pi_g^2$, $\tilde{X}\,^3\Sigma_g^-$.[11–13] With 15 valence electrons, the BO_2, NCO, and N_3 molecules are expected to have $3\sigma_g^2 2\sigma_u^2 1\pi_u^4 4\sigma_g^2 3\sigma_u^2 1\pi_g^3$, $\tilde{X}\,^2\Pi_g$ ground states, as observed.[14–16] In these cases, the existence of three electrons in the $1\pi_g$ orbital inverts the spin-orbit structure, providing an experimental verification of the orbital occupancy. Finally, with 16 valence electrons, the FCN, CO_2, and N_2O molecules complete the filling of the $1\pi_g$ orbital to give $3\sigma_g^2 2\sigma_u^2 1\pi_u^4 4\sigma_g^2 3\sigma_u^2 1\pi_g^4$, $\tilde{X}\,^1\Sigma_g^+$ ground states.

Throughout the range of 11–16 valence electrons, it appears that Walsh's prediction of linear *p*-block molecules is holding up quite well. It remains to be seen if this prediction will remain valid for other electron-deficient molecules, such as BC_2 (also 11 valence electrons) and B_2C (10 e^-). There are strong indications that these molecules may be bent or cyclic,[50–55] as is the case for B_3 (9 e^-).[6]

V. CONCLUSION

A resonant two-photon ionization investigation of the spectroscopy of BNB has identified the $\tilde{B}\,^2\Pi_g - \tilde{X}\,^2\Sigma_u^+$ band system, for which the origin band has been rotationally resolved and analyzed. The analyses for the $^{10}B^{14}N^{11}B$ (mass 35) and $^{11}B^{14}N^{11}B$ (mass 36) isotopomers are consistent with one another, providing ground and excited state B–N bond lengths of 1.3124(1) and 1.3108(1) Å, respectively. The electronic structure of BNB is compared to that of related triatomic molecules and is discussed in relation to Walsh's rules.

ACKNOWLEDGMENTS

This work was supported by the Swiss National Science Foundation, under Project No. 200020-100019. Work performed by one of the authors (M.D.M.) was supported by the U.S. National Science Foundation under Grant No. CHE-0415647.

[1] A. D. Walsh. J. Chem. Soc. 2266 (1953).
[2] G. Herzberg. *Molecular Spectra and Molecular Structure III: Electronic Spectra and Electronic Structure of Polyatomic Molecules* (Van Nostrand Reinhold. New York. 1966).
[3] P. F. Bernath. *Spectra of Atoms and Molecules* (Oxford University Press. New York. 1995).

[4] M. Keil, H. G. Kramer, A. Kudell, M. A. Baig, J. Zhu, W. Demtroder, and W. Meyer, J. Chem. Phys. **113**, 7414 (2000).
[5] D. Bellert, D. K. Winn, and W. H. Breckenridge, J. Chem. Phys. **117**, 3139 (2002).
[6] P. Cias, M. Araki, A. Denisov, and J. P. Maier, J. Chem. Phys. **121**, 6776 (2004).
[7] J. J. Van Vaals, W. L. Meerts, and A. Dymanus, Chem. Phys. **82**, 385 (1983).
[8] A. E. Douglas, Astrophys. J. **114**, 466 (1951).
[9] A. J. Merer and D. N. Travis, Can. J. Phys. **43**, 1795 (1965).
[10] A. J. Merer and D. N. Travis, Can. J. Phys. **44**, 353 (1966).
[11] C. Devillers and D. A. Ramsay, Can. J. Phys. **49**, 2839 (1971).
[12] G. Herzberg and D. N. Travis, Can. J. Phys. **42**, 1658 (1964).
[13] M. C. Curtis, A. P. Levick, and P. J. Sarre, Laser Chem. **9**, 359 (1988).
[14] J. W. C. Johns, Can. J. Phys. **39**, 1738 (1961).
[15] R. N. Dixon, Philos. Trans. R. Soc. London, Ser. A **252**, 165 (1960).
[16] A. E. Douglas and W. J. Jones, Can. J. Phys. **43**, 2216 (1965).
[17] J. K. Tyler and J. Sheridan, Trans. Faraday Soc. **59**, 2661 (1963).
[18] C. P. Courtoy, Ann. Soc. Sci. Bruxelles, Ser. 1 **73**, 5 (1959).
[19] D. K. Coles, E. S. Elyash, and J. G. Gorman, Phys. Rev. **72**, 973 (1947).
[20] H. Habara, A. Maeda, and T. Amano, J. Mol. Spectrosc. **221**, 31 (2003).
[21] G. R. Bird, J. Chem. Phys. **25**, 1040 (1956).
[22] F. X. Powell, J. Chem. Phys. **45**, 1067 (1966).
[23] K. S. Buckton, A. C. Legon, and D. J. Millen, Trans. Faraday Soc. **65**, 1975 (1969).
[24] R. Trambarulo, S. N. Ghosh, C. A. Burrus, Jr., and W. Gordy, J. Chem. Phys. **21**, 851 (1953).
[25] R. D. Brown, F. R. Burden, P. D. Godfrey, and I. R. Gillard, J. Mol. Spectrosc. **52**, 301 (1974).
[26] A. R. W. McKellar, J. B. Burkholder, A. Sinha, and C. J. Howard, J. Mol. Spectrosc. **125**, 288 (1987).
[27] H. J. Bernstein and J. Powling, J. Chem. Phys. **18**, 685 (1950).
[28] L. B. Knight, Jr., D. W. Hill, T. J. Kirk, and C. A. Arrington, J. Phys. Chem. **96**, 555 (1992).
[29] W. Weltner, Jr., *Magnetic Atoms and Molecules* (Dover, New York, 1983).
[30] P. Hassanzadeh and L. Andrews, J. Phys. Chem. **96**, 9177 (1992).
[31] L. Andrews, P. Hassanzadeh, T. R. Burkholder, and J. M. L. Martin, J. Chem. Phys. **98**, 922 (1993).
[32] C. A. Thompson, L. Andrews, J. M. L. Martin, and J. El-Yazal, J. Phys. Chem. **99**, 13839 (1995).
[33] K. R. Asmis, T. R. Taylor, and D. M. Neumark, J. Chem. Phys. **111**, 8838 (1999).
[34] G. Meloni, M. S. Baba, and K. A. Gingerich, J. Chem. Phys. **113**, 8995 (2000).
[35] J. M. L. Martin, J. P. Francois, and R. Gijbels, J. Chem. Phys. **90**, 6469 (1989).
[36] J. M. L. Martin, J. P. Francois, and R. Gijbels, Chem. Phys. Lett. **193**, 243 (1992).
[37] J. M. L. Martin, J. El-Yazal, J. P. François, and R. Gijbels, Mol. Phys. **85**, 527 (1995).
[38] Z.-X. Wang, M.-B. Huang, and P. v. R. Schleyer, J. Phys. Chem. A **103**, 6475 (1999).
[39] S. R. Gwaltney and M. Head-Gordon, Phys. Chem. Chem. Phys. **3**, 4495 (2001).
[40] S. Mahalakshmi and D. L. Yeager, Mol. Phys. **101**, 165 (2003).
[41] A. Kalemos, T. H. Dunning, Jr., and A. Mavridis, J. Chem. Phys. **120**, 1813 (2004).
[42] F. Guthe, H. Ding, T. Pino, and J. P. Maier, Chem. Phys. **269**, 347 (2001).
[43] W. C. Wiley and I. H. McLaren, Rev. Sci. Instrum. **26**, 1150 (1955).
[44] S. Gerstenkorn and P. Luc, *Atlas du Spectre d'Absorption de la Molécule d'Iode entre* 14,800–20,000 cm^{-1} (CNRS, Paris, 1978).
[45] S. Gerstenkorn and P. Luc, Rev. Phys. Appl. **14**, 791 (1979).
[46] R. F. Curl, Jr., Mol. Phys. **9**, 585 (1965).
[47] H. Lefebvre-Brion and R. W. Field, *The Spectra and Dynamics of Diatomic Molecules* (Elsevier, Amsterdam, 2004).
[48] C. M. Western, PGOPHER, a program for simulating rotational structure, University of Bristol, http://pgopher.chm.bris.ac.uk
[49] W. J. Balfour, J. Cao, C. V. V. Prasad, and C. X. W. Qian, J. Chem. Phys. **101**, 10343 (1994).
[50] J. M. L. Martin, P. R. Taylor, J. T. Yustein, T. R. Burkholder, and L. Andrews, J. Chem. Phys. **99**, 12 (1993).
[51] L. B. Knight, Jr., S. Cobranchi, and E. Earl, J. Chem. Phys. **104**, 4927 (1996).
[52] J. D. Presilla-Marquez, C. W. Larson, P. G. Carrick, and C. M. L. Rittby, J. Chem. Phys. **105**, 3398 (1996).
[53] M. Wyss, M. Grutter, and J. P. Maier, J. Phys. Chem. A **102**, 9106 (1998).
[54] J. M. L. Martin and P. R. Taylor, J. Chem. Phys. **100**, 9002 (1994).
[55] C. W. Larson and J. D. Presilla-Marquez, J. Chem. Phys. **111**, 1988 (1999).